

NANOSECOND ACOUSTIC STRAIN PULSES FROM CdS PHONON MASERS

M.D. Smeaton, R.C. Hughes*, J. Vrba**, R.R. Haering
Department of Physics, University of British Columbia
Vancouver, B.C., Canada

Observations of nanosecond strain pulses generated by a mode-locked CdS phonon maser are reported. Peak strains exceeding 5×10^{-5} have been measured. An analogy is drawn between the observed mode-locked operation and a repetitive pulse generator.

In the presence of a D.C. electric field, acoustic cavities, defined by polishing the faces of CdS single crystals accurately flat and parallel, form high Q resonant structures which are strongly analogous to lasers. Maines and Paige¹ reported that CdS phonon maser (PM), operated under certain experimental conditions, exhibited sharp current spiking. The frequency display of the current consisted of a harmonic series having amplitudes constant in time, and a frequency spacing equal to the reciprocal of the round trip transit time of the crystal cavity. From these observations Maines and Paige¹ concluded that the PM was operating in a mode-locked regime, and, by analogy with mode-locked optical lasers, predicted that the acoustic output should consist of narrow, high strain pulses. The validity of this prediction is however, far from obvious, since the mode-locked regime is strongly nonlinear so that there is no one-to-one correspondence between the frequency spectrum of the acoustoelectric current and that of the acoustic fields. When the piezoelectric potential associated with these fields is much larger than the thermal energy, a sinusoidal acoustic wave can result in a strongly nonsinusoidal electron distribution². The strong D.C. current saturation observed in the mode-locked regime indicates that the electrons are constrained to move with the velocity of sound and are thus trapped in the potential wells associated with the acoustic wave. This establishes the strongly nonlinear nature of the mode-locked regime², and suggests that the prediction of Maines and Page¹ should be verified by direct observation of the acoustic fields.

By acoustically coupling a CdS PM to a passive cavity, we have directly observed nanosecond acoustic strain pulses using optical filtering techniques. Our experimental set-up is shown schematically in Fig. 1. The CdS crystal was oriented so that the b-axis was perpendicular to the polished cavity surfaces. For this orientation the active acoustic modes consist of shear waves whose K-vectors lie along the b-axis.

* Present Address: Defence Research Establishment Atlantic
Dartmouth, N.S.

** Present Address: Canadian Thin Films Ltd.
3168 Lake City Way, Burnaby, B.C. V5A 3A4

The R.F. current signal from the active crystal could be displayed either in the frequency regime, by means of a spectrum analyzer, or in the time regime by means of a sampling oscilloscope. The active crystal was coupled to a passive fused quartz cavity by means of a high quality acoustic bond³. Since the two materials have nearly the same acoustic impedance for the chosen CdS orientation, the double cavity modes are nearly harmonic⁴. The passive cavity provides a convenient means of examining the acoustic field of the PM, since high power laser light may be passed through it. Such a high intensity probe may not be used in the active cavity since the large photocurrents produced would disrupt or prevent oscillation.

For our experimental configuration (see Fig. 1) the focal plane diffraction pattern consisted of a vertical row of 30-40 spots symmetrically arranged about the zero order or undiffracted beam. A focal plane spatial filter was used to remove certain diffracted orders before the optical signal was imaged on a 25 micron slit coupled to a photomultiplier. The photomultiplier could be driven transverse to the optical axis, as indicated in Fig. 1, in order to investigate the spatial variation of light intensity in the image plane. The nature of the spatial filter depended upon the particular experiment performed.

Acoustic strains introduce local variations in refractive index, thus presenting a phase grating to the incident light. The relation between the local strain and refractive index variation is linear⁵, so that the phase variation profile of the acoustic grating directly yields the strain profile. If we describe the phase variation of the acoustic cavity by $\Phi(x,t)$, the near field light amplitude, just after passing through the cavity, is given by

$$A(x,z,t) = e^{i\phi(z,t)} e^{i\Phi(x,t)} \approx e^{i\phi(z,t)} [1 + i\Phi(x,t)] \quad [1]$$

where $\phi(z,t) = \omega t - kz$ is the phase of a unit amplitude plane light wave incident on the passive cavity. For the strains we have observed $\Phi(x,t)$ has a maximum value of ~ 0.01 radians which allows one to expand the second exponential in Eq. [1] as shown. If the optical system following the acoustical phase grating is distortion free, then Eq. [1] also applies to the image plane, except for a spatial magnification factor. Since the acoustic cavity alters only the phase of the incident light, the strain field is not directly visible in the image plane. However, removing the zero order or undiffracted beam (represented by the factor 1 in $(1 + i\Phi)$, see Eq. [1]) in the focal plane we obtain the dark field image⁶. In this case phase variations in the object plane produce intensity variations in the image plane. The first order dark field image is

$$I_{DF}(x,t) \approx \Phi^2(x,t) \quad [2]$$

In mode-locked operation the acoustic output of the PM consists of many harmonically related frequency components. The optical phase variation in the passive cavity will then be due to a superposition of an incident wave train coupled from the PM, and a wave train spatially reflected from the free surface ($x = L$) of the passive cavity. Assuming no losses, the resulting phase function may be written in the form

$$\phi(x,t) = \sum_{n=1}^N V_n \{ \sin[nKx - n\Omega t + \alpha_n] + \sin [nK(x-2L) + n\Omega t - \alpha_n] \} \quad [3]$$

where N is the number of active modes and Ω, K are the frequency and wave vector of the fundamental component. The coefficients V_n are Raman-Nath parameters and are proportional to the corresponding strain amplitudes⁵. The set of phases α_n determine the exact profile of the strain pulses. If Eq. [3] is substituted into Eq. [2], the resulting expression may be cast into a form where the various frequency components may be extracted. The D.C. term may then be shown to be

$$I_0 = \sum_{n=1}^N V_n^2 [1 - \cos 2nK(x-L)] \quad [4]$$

Fig. 2(b) shows the experimental image plane intensity variation of the D.C. term for mode-locked PM operation. The corresponding time and frequency displays of the RF current signal are given in Fig. 3. The reciprocal round trip transit time for this particular double cavity corresponded to a fundamental frequency of 325 KHz. By changing voltage and current conditions for the PM, it was possible to vary the frequency separation from this fundamental to about 60 MHz. The separation of the frequency components in Fig. 3(a) is about 11.71 MHz, corresponding to the 36th harmonic of the double cavity fundamental frequency.

The pulse width from Fig. 2(b) is about 23 microns (see caption of Fig. 2 for effective resolution) which corresponds to about 6 nanoseconds for the velocity of sound in fused quartz. Peak strains in excess of 5×10^{-5} have been inferred from typical diffraction intensities. By spatially filtering the diffracted spots corresponding to different frequency orders, we could examine each component of the sum in Eq. [4] individually. In Fig. 2(c) and 2(d), the profiles of the components for $n=1$ and $n=2$ are given. If we choose a reference at a maximum of the $n=1$ component, the cosine components for n odd are found to be (nearly) π out of phase with those for n even, as is predicted by Eq. [4].

While the intensity profile of the D.C. term tells us the strain pulse width, it contains no information about the exact form of the strain profile, since the phases α_n are not present in Eq. [4]. However, our apparatus also allows us to examine the spatial intensity variation of each A.C. term in the image plane. By a combination of spatial and temporal filtering of the optical signal all the phases α_n can, in principle at least, be determined. Preliminary experiments indicate that this determination is practical at least for smaller values of n , where the diffracted intensities are relatively large.

It is useful to make a comparison between the PM operated in a mode-locked regime and a regenerative pulse generator (RPG). It is well known that a feedback loop containing an amplifier, filter, delay line and a saturable absorber behaves as a RPG⁷. In the PM, most of the required elements may be readily identified. The piezoelectric coupling of the acoustic field to drifting electrons provides an amplifying mechanism, a combination of the cavity resonances and the gain profile of the PM constitute the filter, and

the round trip transit time of the resonant cavity serves as the time delay. In the case of an optical laser, which also contains these three basic elements, the saturable absorber must be added to the system for it to function as a RPG⁸. For the PM, however, the saturable absorber is an implicit part of the oscillator itself. Theoretical expressions for acoustic gain as a function of strain amplitude have been derived for piezoelectric semiconductors by Butcher and Ogg^{9,10}. Based on their results for a simple sinusoidal strain⁹, we have obtained an expression for round trip gain in a PM, including lattice and end losses, and have computed theoretical curves for gain vs strain amplitude at the frequency of maximum gain. Such curves indicate that, under typical operating conditions, the net round trip gain increases with strain amplitude. One is thus able to draw a direct analogy between the mode-locked PM and its optical counterpart, the mode-locked laser. For the laser and RPG's in general, the pulse rate is usually equal to the reciprocal of the round trip transit time or loop delay, i.e. there is only one pulse in the system at a time. In our double cavity configuration, the repetition rate was usually some harmonic of the cavity fundamental frequency. An additional distinction may be seen if one considers the product of center frequency and pulse width. A laser pulse having a center frequency of 5×10^{14} Hz ($\lambda = 6000 \text{ \AA}$) and a width of 10^{-12} sec contains 500 optical cycles. On the other hand, our PM has a center frequency of about 10^8 Hz and a pulse width of 6×10^{-9} sec. In both cases the center frequency corresponds to the frequency of maximum gain and the pulse width corresponds to the reciprocal of the bandwidth over which net gain exists. In contrast to an optical laser, the PM produces "D.C." pulses which only contain about 1/2 cycle of the carrier. Such pulses should prove to be of interest in a variety of ultrasonic and acousto-optic applications.

The support of the National Research Council and the Defence Research Board of Canada is gratefully acknowledged.

Figure Captions

- Fig. 1 Configuration for optical experiment. The PM c-axis was perpendicular to the incident light which was provided by an Argon-Ion laser.
- Fig. 2 Intensity variation for D.C. term. On the left are photographs of the image plane optical field. The traces on the right give intensity profiles. Lengths indicated refer to the object plane. The corresponding slit width (resolution) in the object plane is about 1.5 microns. Shown are (a) the bright field image of the double cavity; and dark field images corresponding to (b) all frequency components, (c) $n=1$ component and (d) $n=2$ component.
- Fig. 3 R.F. current signal: (a) frequency display, 20 MHz/div, (b) time display, 10 nanoseconds/div.

References

1. J.D. Maines and E.G.S. Paige, Sol. State Comm. 8, 421 (1970).
2. V.L. Gurevich, Soviet Physics-Semiconductors, 2, 1299 (1969).

3. E.K. Sittig and H.D. Cook, Proc. I.E.E.E. L. 56, 1375 (1968).
4. R.C. Hughes and R.R. Haering, to be published.
5. J. Vrba and R.R. Haering, Can. J. Phys. 51, 1341 (1973).
6. M. Born and E. Wolf, Principles of Optics, Pergamon Press (1959).
7. C.C. Cutler, Proc. I.R.E. 43, 140 (1955).
8. A.J. DeMaria, W.H. Glenn, M.J. Brienza and M.E. Mack, Proc. I.E.E.E. 57, 2 (1969).
9. P.N. Butcher and N.R. Ogg, J. Phys. D. 1, 1271 (1968).
10. P.N. Butcher and N.R. Ogg, J. Phys. D. 2, 333 (1969).

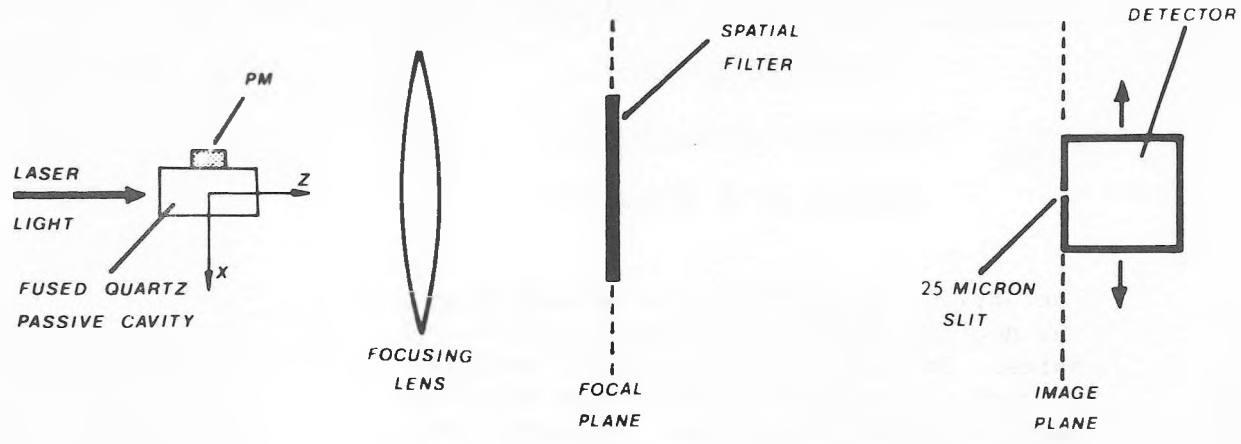


Fig. 1

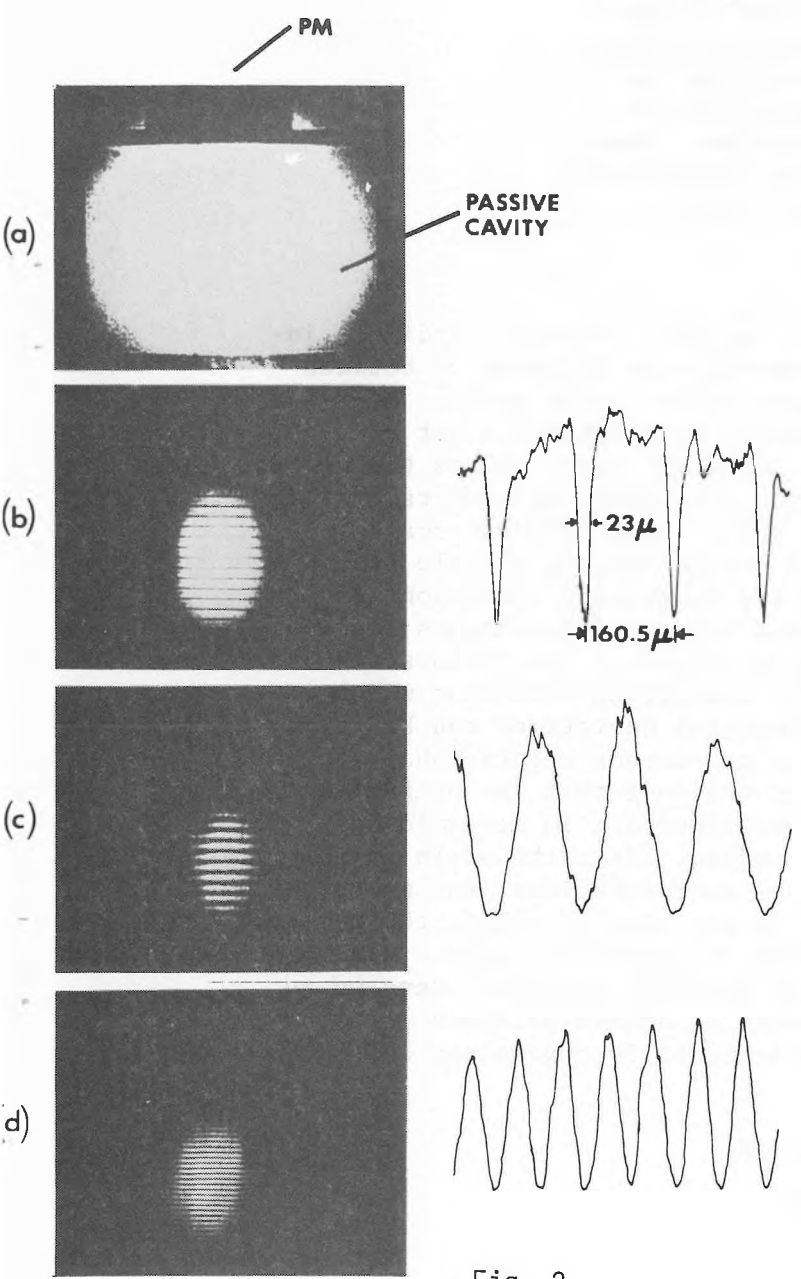


Fig. 2

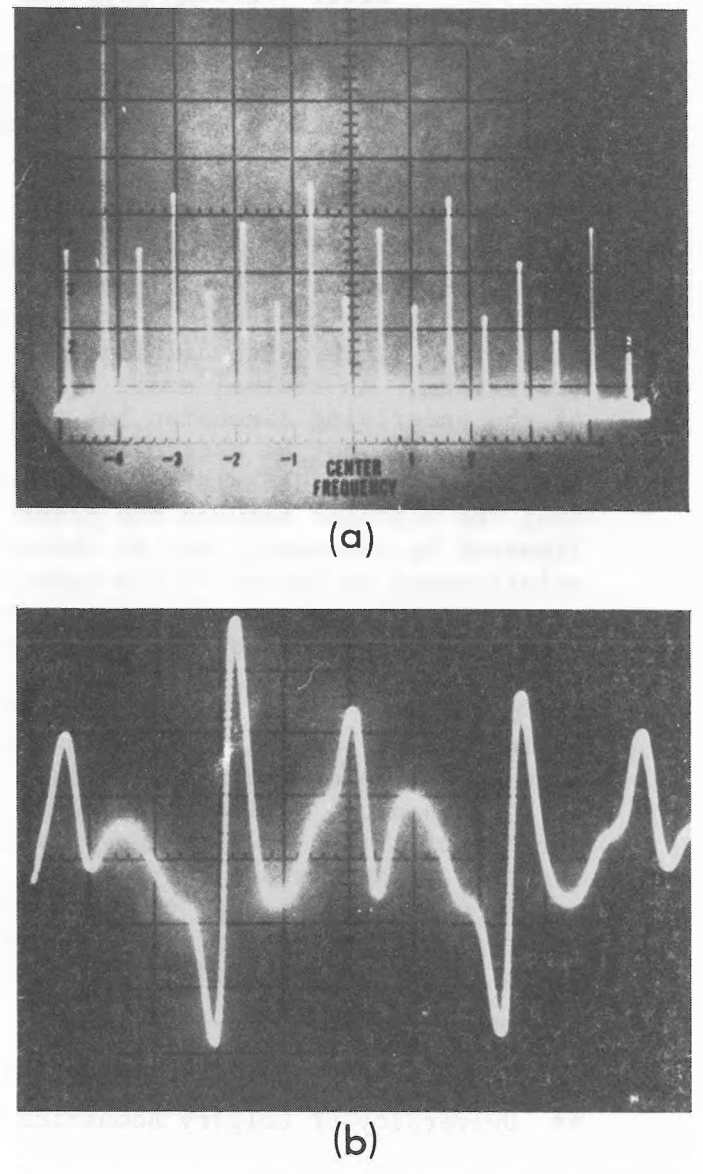


Fig. 3